



Feasibility of a quantum memory for continuous variables based on trapped ions

Thomas Coudreau, Frédéric Grosshans, Samuel Guibal, Luca Guidoni

► To cite this version:

Thomas Coudreau, Frédéric Grosshans, Samuel Guibal, Luca Guidoni. Feasibility of a quantum memory for continuous variables based on trapped ions. 2006. hal-00084554v1

HAL Id: hal-00084554

<https://hal.science/hal-00084554v1>

Preprint submitted on 7 Jul 2006 (v1), last revised 8 Jul 2006 (v2)

HAL is a multi-disciplinary open access archive for the deposit and dissemination of scientific research documents, whether they are published or not. The documents may come from teaching and research institutions in France or abroad, or from public or private research centers.

L'archive ouverte pluridisciplinaire **HAL**, est destinée au dépôt et à la diffusion de documents scientifiques de niveau recherche, publiés ou non, émanant des établissements d'enseignement et de recherche français ou étrangers, des laboratoires publics ou privés.

Feasibility of a quantum memory for continuous variables based on trapped ions

Thomas Coudreau, Frédéric Grosshans, Samuel Guibal, Luca Guidoni

E-mail: coudreau@spectro.jussieu.fr

Laboratoire Matériaux et Phénomènes Quantiques, CNRS UMR 7162, Case 7021,
Université Denis Diderot, 2 Place Jussieu, 75251 Paris cedex 05, France

Abstract. We propose to use a large cloud of cold trapped ions as a medium for quantum optics and quantum information experiments. Contrary to most recent realizations of qubit manipulation based on a small number of trapped and cooled ions, we study the case of traps containing a macroscopic number of ions. We consider in particular the implementation of a quantum memory for quantum information stored in continuous variables and study the impact of the relevant physical parameters on the expected performances of the system.

PACS numbers: 03.67.Hk, 42.50.Lc, 42.50.Ct, 32.80.Pj

Keywords: quantum memories, continuous variables, ion trapping and cooling

1. Introduction

As quantum information becomes closer to applications, the need for quantum memories becomes stronger [1, 2, 3]. Quantum memories are systems which store in so-called "static qubits" the quantum information usually carried by "flying qubits", namely photons. A single ion or a pair of ions forms a prototype of such a quantum memory [4, 5, 6]. It has also been shown that an ensemble of atoms can successfully store the quantum information carried by a single photon [2, 7, 8]. However, quantum information processing is not limited to discrete variables: continuous variable systems also form an attractive tool for such a purpose [9, 10, 11]. In this context, the use of an ensemble of atoms as a quantum memory has been proposed [12, 13] and experimentally demonstrated [14]. In this realization, both the storage medium and the light beam are described by continuous variables.

The goal of this paper is to study the feasibility of a quantum memory relying on a large cloud of cold trapped ions. As we will show, such a system has several advantages with respect to the neutral atom clouds. Among those, one can mention the strong confinement of the ions that opens the way to an efficient interaction with light while keeping the sample immobile in the interaction region for a virtually infinite time. The paper is organized as follows: we will start by describing the basic requisites for a quantum memory and by briefly recalling the principles which govern a light-matter interface suitable for such a purpose. Then, we will propose an experimental implementation based on a cloud of cold trapped ions. We will finally present the expected properties with respect to decoherence and memory lifetime of such a system.

2. Continuous Variable and Quantum Memory Principles

In the case considered here of a quantum memory for continuous variables, quantum information is carried by the quadrature components of a pulse of light such as in [14, 13, 15]. We will quickly recall the continuous variable formalism in subsection 2.1, and then introduce the criteria that define the boundaries between the classical and quantum regimes for a quantum memory in subsection 2.2.

2.1. Continuous Variables

2.1.1. Continuous Observables The observables studied in Continuous Variable quantum systems [16, 17, 18] (the quadratures) are formally analogue to the position and momentum of a particle and hence usually noted \hat{Q} and \hat{P} . In the system described here, the "quadratures" of the ion cloud will be the projection of the global spin of the cloud along some direction, while the corresponding variables of the light beam will be two Stokes operators describing its polarization [19, 20]. When suitably normalized, they obey the canonical commutation relation [16, 17]

$$[\hat{Q}, \hat{P}] = 2i. \tag{1}$$

The above commutation relation implies the Heisenberg relation

$$\delta Q \delta P \geq 1, \quad (2)$$

where δQ (resp. δP) is the standard deviation of Q (resp. P). The fact that the quadratures can take any real value also comes from this commutation relation.

2.1.2. Gaussian States and Channels When the characteristic functions and quasiprobability distributions of the system are Gaussian, it is said to be in a Gaussian state. If Gaussian states are the simplest to study theoretically, they are also fortunately the most common in experiments. We will therefore restrict ourselves to Gaussian states in this article. Since the probability distributions associated with the quadratures of a Gaussian state are Gaussian, such a state is fully characterized by the average value and the covariance matrix of the continuous observables.

A Gaussian operation —*i.e.* an operation which preserves the Gaussian character of the state— can then be described by a linear action on the quadratures, possibly including the coupling with an external mode. For example, the action of a lossy channel with absorption ε on a mode $(\hat{Q}_{\text{in}}, \hat{P}_{\text{in}})$ is given by

$$\hat{Q}_{\text{out}} = \sqrt{1 - \varepsilon} \hat{Q}_{\text{in}} + \sqrt{\varepsilon} \hat{Q}_{\text{vac}} \quad (3)$$

$$\hat{P}_{\text{out}} = \sqrt{1 - \varepsilon} \hat{P}_{\text{in}} + \sqrt{\varepsilon} \hat{P}_{\text{vac}}, \quad (4)$$

where $(\hat{Q}_{\text{vac}}, \hat{P}_{\text{vac}})$ is a mode in a vacuum state *i.e.* \hat{Q}_{vac} and \hat{P}_{vac} are uncorrelated to the input mode, and have zero average value and unit variance.

2.2. Criteria for quantum memory

2.2.1. Generic criteria A quantum memory, by definition, stores informations about a quantum state for a given time interval, and it should do it better than any classical memory (*i.e.* classical-states based memory). Since an *a priori* known quantum state has a complete classical description (its density matrix), it can be reconstructed with an arbitrarily high fidelity by a setup only storing this description in a classical memory. Therefore, similarly to quantum teleportation criteria [21], a quantum memory criterion can only be defined when the input is unknown, *i.e.* when the input state is drawn at random from a given set \mathcal{S} of possible states.

The output of the quantum memory can either be a quantum state or classical information. In the following, we will consider these two situations that we name the *Identity Quantum Memory* (IdQM) and the *Delayed Measurement Quantum Memory* (DMQM). The output of an *Identity Quantum Memory* should be a quantum state as close as possible to the input state. The input-output mapping of a perfect IdQM is then the identity operator, hence its name. Applications of IdQMs include storing intermediate states in quantum computation and the realization of collective attacks against quantum cryptography [22]. The best classical setup devoted to the task of an IdQM, first measures the input state, then stores the obtained information in a classical memory and finally tries to reconstruct the input state from this information.

This reconstruction problem has been well studied and the best classical reconstruction fidelity is well known in a lot of situations [21, 23]. The usual figure of merit for such a memory is the (average or minimal) fidelity, but any distortion measure can be used. Among them, entropic quantities suit to cryptographic applications [22].

While a perfect IdQM allows to construct any conceivable quantum memory, the corresponding criterion, defining the *worst* IdQM, is not always relevant, as shown below.

Another quantum memory application commonly discussed in the literature is related to the delayed measurement problem [24]. A delayed measurement quantum memory (DMQM) receives a quantum state to be stored, and only later learns the measurement to be performed on that state. The output of the DMQM is the classical result of this target-measurement. A commonly discussed application of a DMQM is the realization of individual attacks against quantum cryptographic schemes. As above, the suitable figure of merit changes with the memory application, but, in any case, the fidelity is not the relevant figure of merit, since the output of this quantum memory is classical. The optimal classical strategy to perform a classical measurement is to immediately measure the quantum state and store the result in a classical memory. When the target-measurement is drawn from a set of incompatible measurements, the best classical measurement will be approximative, since it has to guess the result of all incompatible target-measurement. However, this optimal classical strategy doesn't need to reconstruct the input state, which usually renders the criterion for DMQM stricter than the IdQM one. In other words, if an IdQM followed by the relevant measurement is a possible way to build a DMQM, the resulting DMQM is not guaranteed to be better than its optimal classical counterpart, even if the IdQM is above the quantum threshold.

The two definition above can be formalized in a more general framework, described below. A quantum memory is a channel taking two inputs, one of which is a quantum state drawn from a known set $\mathcal{S} = \{\rho_i\}_i$ with probability p_i , and the other is an (optional) delayed information τ . The action of the memory on ρ can be described by the completely positive map ϕ_τ , which should be as close as possible to a target map $\phi_\tau^{\text{target}}$. The target map corresponding to the IdQM described above is the identity $\phi_\tau^{\text{target}} = \mathbb{I}$ and doesn't depend on τ . For the DMQM, the $\phi_\tau^{\text{target}}$ correspond to the various measurements, each τ identifying a particular measurement.

The optimal classical strategy trying to simulate $\phi_\tau^{\text{target}}$ defines the criterion for a quantum memory. This strategy should be based on measurements, classical memory and state reconstruction. Furthermore, the measurements must not depend on τ .

One can see from the above examples and definitions that there are as many criteria for quantum memories as there are applications, the criteria depending on the input state set \mathcal{S} , the target map ϕ_τ , and the chosen figure of merit.

2.2.2. Continuous Variable quantum memories As mentioned before, we will restrict ourselves to continuous variables-quantum memories (IdQM and DMQM). Furthermore,

we will restrict ourself to gaussian quantum memories[‡]. Therefore \mathcal{S} is a covariant set of gaussian states with uniform distribution in phase-space.

Since the quantum memory is gaussian, it can be described like a Gaussian Channel, with the following input-output relation :

$$\hat{Q}_{\text{out}} = \sqrt{G_Q} \hat{Q}_{\text{in}} + \sqrt{N_Q} \hat{Q}_{\text{vac}} \quad (5)$$

$$\hat{P}_{\text{out}} = \sqrt{G_P} \hat{P}_{\text{in}} \pm \sqrt{N_P} \hat{P}_{\text{vac}}, \quad (6)$$

with $N \geq |G - 1|$, where the noise $N = \sqrt{N_Q N_P}$ and the gain $G = \sqrt{G_Q G_P}$.

In the following, we will describe the criteria for IdQM and DMQM, illustrating them *via* the example of an optical fiber loop.

The best classical IdQM approximation is well studied since the early days of continuous variable teleportation [21], and has a unity gain and a noise equivalent to twice the shot noise on both quadratures. An IdQM should therefore verify

$$G_Q = G_P = 1 \quad N < 2. \quad (7)$$

Note that if $G_Q \neq G_P$ but $G = 1$, the memory squeezes the input. Since the squeezing is a reversible operation, such a memory can be considered as a generalized IdQM.

As easily seen from eq. 4, the noise added by an optical fiber of transmission $T = 1 - \varepsilon$ has a variance equal to $\varepsilon = 1 - T$. If one wants to use this fiber as an IdQM, one needs to correct for the transmission gain T by preamplifying the input with a gain $1/T$, adding a noise of at least $1/T - 1$. The resulting channel has then the wanted unit gain, and a noise $N = 2(1 - T)$, always smaller than the classical limit of 2. However, T decreases exponentially, at a rate of 0.04 dB/ μs in a fiber of refracting index $n = 1.5$ and attenuation 0.2 dB/km. The transmission T being divided by 100 every 500 μs , this memory quickly becomes indistinguishable from a classical memory, even in the absence of technical noise.

The canonical continuous variable DMQM allows to measure either Q or P . The corresponding optimal classical measurement has been studied since Heisenberg, and the noise added by this measurement obeys the uncertainty relationship $\delta Q \cdot \delta P \geq 1$. The violation of this relationship, written

$$\frac{N}{G} < 1 \quad (8)$$

is therefore a criterion for continuous variable DMQM.

If one implements a DMQM with a fiber loop followed by a (perfect) homodyne measurement, the relevant figure of merit is the equivalent input noise N/G [16] of the fiber, and the criterion can be written

$$\frac{1}{T} - 1 < 1 \Leftrightarrow T > \frac{1}{2},$$

which corresponds to a maximal storage time of 75 μs in an optical fiber loop.

[‡] even if they are not always optimal for commonly used figures of merit [23]

2.3. Quantum memory with an X-type level scheme

2.3.1. Light-matter interaction The unique experimental realization of a continuous variable quantum memory to date is based on a three step process [14]: first, the light pulse carrying the quantum information is sent through the sample; the output beam is then measured; and finally a feed-back is performed on the sample conditioned on this measurement. In this realization, the levels involved are considered as an X-type system, with two levels in the ground state and two in the excited state coupled by two lasers (Fig. 1). Other level schemes have also been proposed. For instance, when a Λ -type level scheme is used (with only one excited state and two lasers), a single interaction is sufficient [13, 15]. Other proposed schemes, involve multiple passages through the atomic medium [25] and no back-action *via* a magnetic field pulse. In this paper, we will focus on the first scheme.

We will follow here the formalism introduced in [19]. Let us begin by recalling its main properties. The medium consists in N_a atoms with a $1/2 \rightarrow 1/2$ transition coupled to a laser beam close to resonance (figure 1). We consider that the information is carried in a pulse with duration T , much larger than the atomic response time that propagates along the z direction. We denote N_p the total number of photons contained in the pulse.

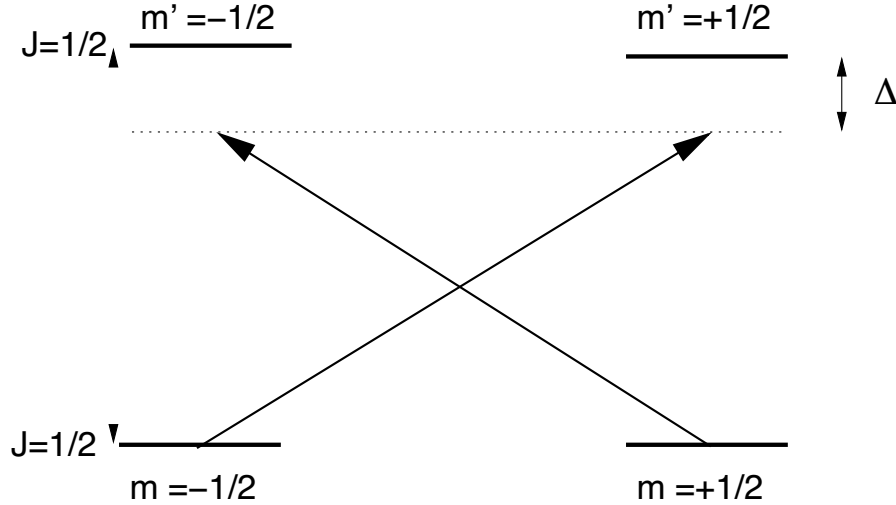


Figure 1. X-type level scheme of the atomic medium used in the quantum memory. The laser is detuned by Δ with respect to a $1/2 \rightarrow 1/2$ transition characterized by a pulsation ω and excited-state lifetime $1/\gamma$.

The basic idea is that the quantum information stored in the polarization state described by quantum Stokes operators is coupled *via* the Faraday effect to the spin operators that characterize the collective spin of the atomic medium.

The collective spin operators of the atomic medium read

$$\hat{J}_{x,y,z} = \sum_{i=1}^{N_a} \hat{\sigma}_{x,y,z}^{(i)} \quad (9)$$

where $\hat{\sigma}_{x,y,z}^{(i)}$ denotes the individual spin of atom i . The light field is described by its quantum Stokes operators [26]:

$$\begin{aligned}\hat{S}_0 &= \hat{a}_x^\dagger \hat{a}_x + \hat{a}_y^\dagger \hat{a}_y \\ \hat{S}_1 &= \hat{a}_x^\dagger \hat{a}_x - \hat{a}_y^\dagger \hat{a}_y \\ \hat{S}_2 &= \hat{a}_x^\dagger \hat{a}_y + \hat{a}_y^\dagger \hat{a}_x = \hat{a}_{+45^\circ}^\dagger \hat{a}_{+45^\circ} + \hat{a}_{-45^\circ}^\dagger \hat{a}_{-45^\circ} \\ \hat{S}_3 &= i(\hat{a}_y^\dagger \hat{a}_x - \hat{a}_x^\dagger \hat{a}_y) = \hat{a}_{\sigma^+}^\dagger \hat{a}_{\sigma^+} + \hat{a}_{\sigma^-}^\dagger \hat{a}_{\sigma^-}\end{aligned}\quad (10)$$

where $\hat{a}_{x,y,\pm 45^\circ,\sigma^\pm}$ and $\hat{a}_{x,y,\pm 45^\circ,\sigma^\pm}^\dagger$ denote respectively the annihilation and creation operators in the horizontal, vertical, $\pm 45^\circ$, left- and right-circular polarizations. The \hat{S}_i and \hat{J}_k operators verify the usual commutation relations:

$$[\hat{S}_1, \hat{S}_2] = i\hat{S}_3 \quad [\hat{J}_x, \hat{J}_y] = i\hat{J}_z, \quad (11)$$

$$[\hat{S}_2, \hat{S}_3] = i\hat{S}_1 \quad [\hat{J}_y, \hat{J}_z] = i\hat{J}_x, \quad (12)$$

$$[\hat{S}_3, \hat{S}_1] = i\hat{S}_2 \quad [\hat{J}_z, \hat{J}_x] = i\hat{J}_y. \quad (13)$$

We consider an input beam linearly polarized along the horizontal direction, so that

$$\langle \hat{S}_1 \rangle = N_p, \langle \hat{S}_2 \rangle = 0 = \langle \hat{S}_3 \rangle.$$

We likewise consider an atomic cloud initially polarized in the x direction (for instance by optical pumping), so that

$$\langle \hat{J}_x \rangle = N_a, \langle \hat{J}_y \rangle = 0 = \langle \hat{J}_z \rangle.$$

One can then define two pairs of operators associated with the light beam and with the atomic sample,

$$\begin{aligned}\hat{Q}_p &= \frac{\hat{S}_2}{\sqrt{\langle \hat{S}_1/2 \rangle}} \quad \text{and} \quad \hat{P}_p = \frac{\hat{S}_3}{\sqrt{\langle \hat{S}_1/2 \rangle}}, \\ \hat{Q}_a &= \frac{\hat{J}_y}{\sqrt{\langle \hat{J}_x/2 \rangle}} \quad \text{and} \quad \hat{P}_a = \frac{\hat{J}_z}{\sqrt{\langle \hat{J}_x/2 \rangle}}.\end{aligned}$$

If we consider that the interaction is weak, one can treat \hat{S}_1 and \hat{J}_x classically so that the above operators verify the canonical commutation relations

$$[\hat{Q}_p, \hat{P}_p] = 2i \quad \text{and} \quad [\hat{Q}_a, \hat{P}_a] = 2i.$$

If we consider a non resonant interaction ($\Delta \gg \gamma$), an input-output relation through the medium can be written as [19]

$$\hat{Q}_p^{(out)} = \sqrt{1 - \varepsilon_p} \left(\hat{Q}_p^{(in)} + \kappa \hat{P}_a^{(in)} \right) + \sqrt{\varepsilon_p} \hat{Q}_p^{(vac)} \quad (14)$$

$$\hat{Q}_a^{(out)} = \sqrt{1 - \varepsilon_a} \left(\hat{Q}_a^{(in)} + \kappa \hat{P}_p^{(in)} \right) + \sqrt{\varepsilon_a} \hat{Q}_a^{(vac)} \quad (15)$$

$$\hat{P}_p^{(out)} = \sqrt{1 - \varepsilon_p} \hat{P}_p^{(in)} + \sqrt{\varepsilon_p} \hat{P}_p^{(vac)} \quad (16)$$

$$\hat{P}_a^{(out)} = \sqrt{1 - \varepsilon_a} \hat{P}_a^{(in)} + \sqrt{\varepsilon_a} \hat{P}_a^{(vac)} \quad (17)$$

where

$$\varepsilon_a = N_p |g|^2 \frac{\gamma}{\Delta^2} \text{ and } \varepsilon_p = N_a |g|^2 \frac{\gamma}{\Delta^2},$$

can be interpreted as the atomic and photonic losses,

$$\kappa = 2\sqrt{N_p N_a} \frac{|g|^2}{\Delta},$$

is the beam-sample coupling constant, $Q_{a,p}^{(vac)}$ and $P_{a,p}^{(vac)}$ are entering noise with a shot-noise limited variance; the atom-photon coupling constant is given by

$$|g|^2 = \frac{3c\lambda^2}{16\pi^2 A} \gamma$$

where A is the beam cross section and λ the transition wavelength.

After such an interaction, the \hat{P}_p quadrature of light has been mapped onto the \hat{Q}_a quadrature of the cloud (see Eq. 14). A second operation is now necessary to map the other quadrature of light onto the other quadrature of the collective spin. As stated previously, this is done using a measurement of the output light beam and a feed back onto the memory.

2.3.2. Measurement and feed-back Using standard quantum optics techniques, one can easily measure the \hat{Q}_p quadrature of the light beam emerging from the cloud. This information can then be mapped onto the atomic operator \hat{P}_a using for example a radio-frequency magnetic field pulse [14]. This can be done using a gain $\sqrt{\mathcal{G}}$ which can be fixed arbitrarily. One has then

$$\begin{aligned} \hat{P}_a^{mem} &= \hat{P}_a^{out} + \sqrt{\mathcal{G}} \hat{Q}_p^{out} \\ &= \sqrt{1 - \varepsilon_a} (1 + \sqrt{\mathcal{G}} \kappa) \hat{P}_a^{(in)} + \sqrt{\mathcal{G}} \sqrt{1 - \varepsilon_p} \hat{Q}_p^{(in)} + \\ &\quad \left(\sqrt{\varepsilon_a} \hat{P}_a^{(vac)} + \sqrt{\mathcal{G}} \sqrt{\varepsilon_p} \hat{Q}_p^{(vac)} \right) \end{aligned}$$

In order to cancel the atomic input noise, $\hat{P}_a^{(in)}$, one can fix $\sqrt{\mathcal{G}} \kappa = -1$ which yields

$$\hat{P}_a^{mem} = -\frac{\sqrt{1 - \varepsilon_p}}{\kappa} \hat{Q}_p^{(in)} + \hat{P}_a^{vac} \quad (18)$$

with

$$\hat{P}_a^{vac} = \sqrt{\varepsilon_a} \hat{P}_a^{(vac)} - \frac{\sqrt{\varepsilon_p}}{\kappa} \hat{Q}_p^{(vac)}.$$

Through these successive operations, the atomic medium quadratures (\hat{Q}_a, \hat{P}_a) contain a term proportional to the input light quadratures (\hat{Q}_l, \hat{P}_l) . We have thus realized a quantum memory for light.

2.3.3. Quantum memory criteria The criteria for an IdQM (Eq.7) and for a DMQM (Eq.8) are expressed as a function of the gains $G_{Q,P}$ and added noises $N_{Q,P}$. In the case studied here, one has

$$G_Q = \kappa^2 (1 - \varepsilon_a) \quad (19)$$

$$G_P = \frac{1 - \varepsilon_a}{\kappa^2} \quad (20)$$

for the gains since the sign in Eq. 18 is not relevant. One also has

$$N_Q = 1 \tag{21}$$

$$N_P = \varepsilon_a + \frac{\varepsilon_p}{\kappa^2} \tag{22}$$

since we assume all the input noises to be uncorrelated and shot-noise limited.

Based on these parameters, we will discuss the feasibility of an ion based memory in Sec. 4.3. We now turn our attention to the experimental implementation that we propose, based on a large ensemble of cold ions with a $1/2 \rightarrow 1/2$ transition efficiently coupled to light.

3. Experimental implementation

3.1. Linear Paul trap

Trapping particles with external fields allows to produce well controlled quantum systems isolated from the environment. Furthermore, laser cooling techniques have brought the possibility of creating dilute gases with extremely narrow velocity distributions, thus optimizing the interaction with optical fields and the control of the system by these fields. A standard tool to trap and manipulate neutral atoms is the Magneto-Optical Trap (MOT)[36]. In such traps, the atomic sample has to be in permanent interaction with near-resonance lasers in order to remain trapped. This interaction induces a high rate of spontaneous emission, leading to a rapid decoherence of both external and internal degrees of freedom. Cold atoms based quantum-optics experiments are thus usually carried out in the absence of the cooling and trapping lasers on a free sample, leading to relatively short interaction times (ms) and evolving conditions (velocity, density...) [37]. The ion trapping techniques take advantage of the strong electrostatic force which allows one to tailor very deep (eV) confining potentials that are independent of cooling lasers. The laser cooling techniques can be applied very efficiently to the trapped sample, with a very simple 1D beam geometry that performs 3D cooling due to the strong coupling of the motional degrees of freedom induced by the electrostatic forces between ions. Once cooled, the ions may remain trapped and cool in the absence of cooling lasers for long period of time (s) compared to atom traps. A standard tool for trapping ions in quantum optics and quantum information experiments is the Paul trap that is based on time-varying electric potential applied to a set of electrodes. The standard Paul trap [38] has a quasi-spherical geometry with few optical access. A common variant is the linear-Paul trap [39], based on the same principles but offering more versatility in the geometry design. In order to carry-out quantum memory experiments involving the macroscopic spin of an ion sample, it is important to optimise the interaction of a laser beam with the sample. Thus, we have chosen a very anisotropic geometry, leading to quasi-1D sample, very elongated along the propagation direction of the laser (z). The linear-Paul trap (Figure 2) is made of four rods as main trapping electrodes, two of them being brought to a high-frequency high-voltage potential. These electrodes are responsible for a 2D confinement in the

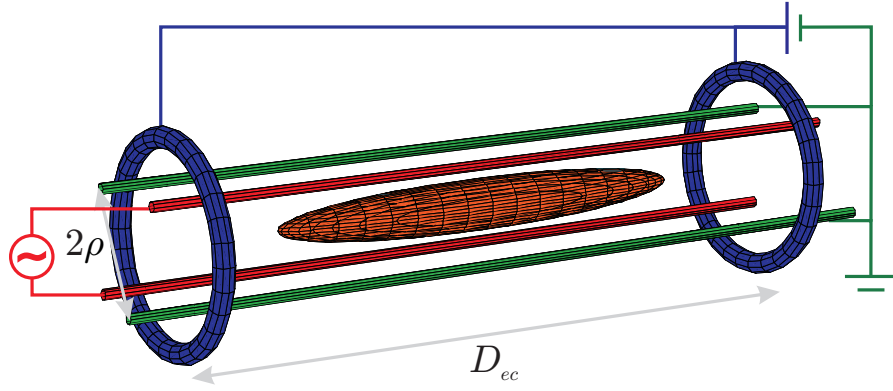


Figure 2. Principle of a linear Paul trap. Two transverse trapping electrodes are brought to a high-frequency high-voltage potential (in red), two are at ground voltage (green). The longitudinal trapping electrodes are brought to a static positive voltage (blue). The ions are trapped as an ellipsoidal cloud at the center of the trap (orange).

plane (xOy) perpendicular to the electrodes axis. Two ring electrodes brought to a static positive voltage trap the ions along the axial direction (Oz).

This geometry offers a wide variety of optical accesses, in transverse direction for laser cooling and along the axis for optimal interaction with a focused laser beam carrying the quantum information. This set-up is currently being developed in our group. The dimension we have chosen ($\rho = 2.6$ mm, $D_{ec} = 20$ mm, see Fig. 2) allows the formation of a sample of 5 mm long, $200\ \mu\text{m}$ large, containing a few 10^5 ions [28]. Using a tighter confinement, *i.e.* more closely spaced electrodes, one can expect to trap approximately $2.2 \cdot 10^6$ ions using realistic values for the RF voltage (800 V) with a section of $60\ \mu\text{m}$ and a length of 2 cm for the ions cloud.

3.2. Choice of the ion

We restrict ourselves to the second column of the periodic table (alkaline earth elements) : these elements, when deprived of an electron, have an electronic structure consisting of a shell with a single orbiting electron. This structure, identical to the alkaline elements, readily provides transitions necessary for an easy manipulation with light fields. The available non radioactive elements are beryllium, magnesium, calcium, strontium and baryum. All these ions have identical electronic structures namely $2S_{1/2} \rightarrow 2P_{1/2}$ transitions. These transitions are located from the mid (Be^+) to the near UV (Ba^+). Choosing the last two elements allows one to use solid-state laser technologies, such as Ti:Sa lasers. It is interesting to choose two neighboring species (like Sr^+ and Ba^+) which can be easily manipulated with light fields: having two species at hand allows one to perform sympathetic cooling [29]. In a sympathetic cooling scheme, the heavier element (Ba^+) will be located at the perimeter of the trap and the lighter element (Sr^+) at the center. This last element will thus be confined in an elliptic-shaped region, well adapted to the interaction with a focused laser beam. In the following, we will thus consider a cloud of cold Sr^+ ions as active medium.

4. Trapped ions for a quantum memory

4.1. Relevant parameters for the X-type level scheme

As mentioned in section 2.3, the relevant parameters are κ and $\varepsilon_{a,p}$. We first compare on Tab.1, the values of the experimental parameters for the proposed experiment and that used in [14].

	N_p	N_a	λ (nm)	Δ (MHz)	γ (MHz)	A (cm ²)
Ref. [14]	$4 \cdot 10^{12}$	$3 \cdot 10^{11}$	852	700	5	6
Ion cloud	$< 10^{12}$	$1.5 \cdot 10^6$	422	> 100	20	$8 \cdot 10^{-9}$

Table 1. Experimental parameters

From these values, one can calculate the parameters relevant for Eqs. (14-17): the corresponding values of g , κ and $\varepsilon_{a,p}$ are shown in Tab. 2. The calculation of these parameters for experiment [14] is more involved since the transition which is used is $F = 4, m_F = \pm 4 \rightarrow F' = 5$. Thus we will use the value for κ given in Ref.[14]. In this experiment, the number of photons and atoms involved being large, the noises induced by $\varepsilon_{a,p}$ are small (the value given by our model are indicated in Tab. 2 as a reference). The exact values of ε_p is not relevant since the optical losses due to the cell windows are predominant.

	g^2	κ	ε_a	ε_p
Ref. [14]	$34.5 \cdot 10^3$	0.37	$5 \cdot 10^{-3}$	$3.5 \cdot 10^{-4}$
Ion cloud	$1.8 \cdot 10^9$	0.64	0.09	$1.4 \cdot 10^{-8}$

Table 2. Relevant parameters for light-matter interface. For the ion experiment, we have taken $N_p = 2.1 \cdot 10^{12}$ (corresponding to the same power as Ref.[14]), $N_a = 1.5 \cdot 10^6$, $\Delta = 8 \cdot 10^3 \gamma$, $A = 1.1 \cdot 10^{-8} \text{ m}^2$ (corresponding to a beam waist of $60 \mu\text{m}$, adjusted to the maximal cloud section).

One remarks that, even though the values of κ are comparable, the photonic noise term, due to ε_p , is much larger in the ion experiment. This is due to the fact that the number of interacting atoms, N_a , is much smaller in this experiment. The use of an immobile ensemble of ions allows one to choose a much tighter focusing, increasing the atom-photon coupling constant, g and keeping the value of κ large. Furthermore, let us note that the value of ε_a remains very small, on the order of a few percent, which is comparable to the other losses which will appear in a typical quantum optics experiments (detection losses in particular). One also remarks that ε_a and κ both depend on the ratio N_p/Δ^2 . When this quantity is kept constant, ε_a and κ will both remain constant (provided the other parameters do not change). One can thus use a much smaller number of photons, for instance using shorter pulses (μs), together with

a smaller detuning. This approach remains valid as long as N_p remains larger than N_a : when $N_a \gg N_p$, the dominant noise is the photonic noise corresponding to ε_p .

4.2. Performances of the memory, decoherence

Let us now discuss the behavior of the proposed ion memory with respect to the decoherence and other phenomena that may affect its performances. We can distinguish three different phases in which a real memory may not follow an ideal behavior: the writing phase, the storage phase and the readout phase. We discussed in section 2.2.2 the effect of the losses ε associated to the writing and (eventually) to the readout phases. In particular, in the case of a DMQM the condition $\varepsilon < 1/2$ must be fulfilled, where we consider ε as the cumulative losses. Concerning the volatility of the memory, the decoherence of the collective spin state is the main limitation to long storage times. Such a decoherence can be described in terms of an additional loss ε_{sto} that takes into account the spins flips or atomic losses that may occur in the cloud. In the neutral-atom based memory [14] the storage time is limited by three major phenomena: the spin-flips that can occur during atomic collisions, the finite time spent by an atom in the laser beam, and the dephasing induced by magnetic field inhomogeneities. The first two phenomena are expected to give a negligible contribution in the case of cold trapped ions. Indeed, due to the electrostatic repulsion, the ions can not collide to give a spin-flip (core collisions): in a raw evaluation the spin-spin and spin-orbit interaction at the characteristic distance of $\simeq 1\mu\text{m}$ can only affect the energy levels with a shift of the order of 100 Hz [30]. Furthermore, the ion cloud being trapped by electrostatic fields that confine strongly the ion cloud and which are not switched-off during the experiment, no ion will move out of the laser beam during the whole interaction time.

The main effect of magnetic field inhomogeneities is to induce a spread in the precession frequencies around the external magnetic field that imposes the quantification axis. Such an effect would seem to affect an ion cloud in the same way it affects a neutral atomic cloud. However, in an ion Coulomb crystal the position of every ion is fixed in space. In this situation, when the readout time for the information stored in the quantum memory is a known parameter, it is possible to wash-out the effect of inhomogeneities with a spin-echo experiment. Moreover, let us remark that the space region in which the inhomogeneities have to be controlled is smaller in the case of trapped ions: it is therefore easier to use passive or active compensation coils to reduce the stray fields down to some tenths of nT [31].

Let us now discuss the other phenomena that could deteriorate the performances of a quantum memory in the case of trapped ion clouds. Large ion Coulomb crystal can be obtained with characteristic temperatures in the range of 20–100 mK [32, 33]. Contrary to the case of ions near the trap axis, the ions in the external part of the crystal are subject to a non-vanishing RF field that induces a micro-motion. In a laser-cooled sub-Kelvin crystal, such a micro-motion, that mainly affects the radial motion of the ion, is not the main source of heating [33] and its effect is mainly limited to a Doppler

Shift of the optical transition (that is important only during the writing and reading phases). This residual motion is well described by a thermal motion with a maximum temperature in the 100 mK range, that gives us for Sr^+ a rms Doppler shift of ~ 10 MHz, much smaller than the detuning Δ and smaller than the natural line-width γ . Let us remark again that the situation of a large ion cloud described by a collective continuous quantum variable is very different with respect to the case of discrete motional quantum states that are very sensitive to any residual micro-motion. Other contributions to the decoherence could originate from the DC Stark shift induced by trapping electric fields and from the quadrupolar shift due to electric-field gradients. The first contribution should vanish at the potential minima that correspond to equilibrium position in an ion crystal, but the ions are subject to thermal motion and explore regions with nonzero fields and gradients. Such a problem has been carefully analyzed in the case of single ions trapped in the center of a small trap for metrology purposes [34, 35]. In this case the main contribution to the shift of energy levels is the quadrupolar coupling that, for well compensated traps can be as low as a fraction of Hz. Even in a larger trap, we still expect a negligible contribution to decoherence from these phenomena. Finally, another candidate that could affect the storage time of an ion-based memory is the presence of collisions with the neutral background gas in the vacuum chamber. This phenomenon is the most important heating source in large cold Coulomb crystals [33]: the trapped ions that collide with a neutral particle are not ejected from the trap but their kinetic energy increases such that they escape from their initial site. Such kind of collisions could naturally induce a spin-flip and their rate should be minimized in order to achieve long storage times. The expected rates in ion Coulomb crystals in a vacuum of $\simeq 10^{-10}$ mbar are of the order of $\frac{1}{\tau} = 0.03$ collisions per ion per second [29]. Such a rate will induce an exponential time-dependent loss term $\varepsilon_{sto}(t) = 1 - \exp(-2t/\tau)$.

4.3. Quantum memory criteria

As shown previously, the quality of the quantum memory can not be evaluated independently of its purpose. It is thus necessary to calculate the parameters $G = \sqrt{G_Q G_P}$ and $N = \sqrt{N_Q N_P}$. These parameters can be calculated taking into account additional optical losses before and after the interaction as well as the decay induced by the main cause of decoherence, *i.e.* collisions with neutral particles as mentioned above.

Taking $\Delta = 3 \cdot 10^4 \gamma$ and no losses, one gets $N = 0.08$ and $G = 1$ without losses. If one takes into account the losses, G is now 0.96 and N is 1.6. The criteria for a generalized IdQM ($G = 1$, $N < 2$) is thus fulfilled for N but not for G except in the absence of losses. This system is thus not suitable for such an application.

However, it forms a very efficient DMQM, as we will show. We calculate now the values of G and N in different cases (Tab. 3).

This table shows N/G is small in both cases. We remark that the value expected for the ion cloud is smaller with respect to the value obtained for Ref.[14]. We also show that the storage time during which the memory keeps its quantum character is on the

	G	N	$\frac{N}{G}$
Ioncloud, nolosses	0.90	0.31	0.33
Ioncloud, losses, $t = 0$ s	0.88	0.52	0.60
Ioncloud, losses, $t = 9$ s	0.67	0.67	1.0
Ref. [14]	0.84	0.67	0.80

Table 3. Quantum memory parameters. The optical losses in the ion experiment are taken to be equal to 1% before the interaction and 5% after, reflecting the detection losses. In experiment [14], we take the losses to be evenly distributed before and after the interaction and corresponding to the 8 uncoated optical windows present in the experiment.

order of 9 s, very long compared to the storage times previously demonstrated.

Let us also mention the use of ion clouds in the Λ -type scheme performed inside a cavity [13]. The relevant parameter for such an experiment is the so-called cooperativity parameter C defined as

$$C = \frac{2\pi g^2 N_a}{c\gamma T} \quad (23)$$

where T is the coupling mirror intensity transmission and the other parameters have been previously defined. Using a typical value $T = 0.1$ for the coupling mirror transmission, one obtains for our parameters $C \approx 55$ which is similar to the value typically obtained with cold neutral atoms in a magneto-optical trap.

Our analysis demonstrate that, independently of the chosen interaction scheme, a quantum memory based on a cold ion cloud is feasible. Moreover, this approach leaves open for the experimentalist the possibility to explore a wide region in the parameter space, still obtaining a functional memory.

5. Conclusion

In this paper we presented the theoretical and practical issues related to the realization of a quantum memory that stores quantum information carried by continuous variables in the collective spin observables of a large cloud of trapped and cooled ions. In particular we discussed the different criteria that quantum memories may have to fulfill and we presented the physical basis of quantum recording, based on previous theoretical analysis [19]. By comparing the relevant physical parameters that can be obtained using a large ion crystal to that of the unique experimental example of an atomic quantum memory [14], we demonstrated that the use of laser cooled ions (e.g. $^{88}\text{Sr}^+$ ions) is, under several aspects, an ideal case. We discussed the phenomena that affect the performances of this

quantum memory and we concluded that a ion Coulomb-crystal based memory is feasible and that it will probably outperform the neutral-atom based quantum memories.

acknowledgement

Laboratoire Matériaux et Phénomènes Quantiques of the Université Denis Diderot is associated with the Centre National de la Recherche Scientifique, UMR CNRS 7162.

We acknowledge fruitful discussions with M. Pinard.

- [1] D.P. DiVincenzo, *"The Physical Implementation of Quantum Computation"*, Fortschr. Phys. **48**, 771-783 (2000)
- [2] L.M. Duan, M. Lukin, J.I. Cirac, P. Zoller, *"Long distance quantum communication with atomic ensembles and linear optics"*, Nature **414**, 413 (2001)
- [3] M.D. Lukin, *"Trapping and manipulating photon states in atomic ensembles"*, Rev. Mod. Phys. **75**, 754-777 (2003).
- [4] D. Kielpinski, V. Meyer, M. A. Rowe, C. A. Sackett, W. M. Itano, C. Monroe, and D. J. Wineland, *"A Decoherence-Free Quantum Memory Using Trapped Ions"*, Science **291**, 1013 (2001)
- [5] B. B. Blinov, D. L. Moehring, L.- M. Duan and C. Monroe, *"Observation of entanglement between a single trapped atom and a single photon"*, Nature (London) **428**, 153 (2004)
- [6] C. Langer, R. Ozeri, J. D. Jost, J. Chiaverini, B. DeMarco, A. Ben-Kish, R. B. Blakestad, J. Britton, D. B. Hume, W. M. Itano, D. Leibfried, R. Reichle, T. Rosenband, T. Schaetz, P. O. Schmidt, D. J. Wineland, *"Long-lived qubit memory using atomic ions"*, Phys. Rev. Lett. **95**, 060502 (2005)
- [7] T. Chaneliere D. N. Matsukevich, S. D. Jenkins, S.-Y. Lan, T. A. B. Kennedy, A. Kuzmich, *"Storage and retrieval of single photons transmitted between remote quantum memories"*, Nature **438**, 833 (2005)
- [8] C. W. Chou, H. de Riedmatten, D. Felinto, S. V. Polyakov, S. J. van Enk, H. J. Kimble, *"Measurement-induced entanglement for excitation stored in remote atomic ensembles"*, Nature **438**, 828 (2005)
- [9] Quantum information with Continuous Variables, edited by S. L. Braunstein and A. K. Pati (Kluwer Academic Publishers, Dordrecht, 2003)
- [10] S. L. Braunstein and P. van Loock, *"Quantum information with continuous variables"*, Rev. Mod. Phys. **77**, 513 (2005).
- [11] Quantum Information with Continuous Variables of Atoms and Light, N.Cerf, Leuchs and Polzik eds. Imperial College Press in press (2005).
- [12] A. E. Kozhekin, K. Mølmer, and E. Polzik, *"Quantum memory for light"*, Phys. Rev. A **62**, 033809 (2000)
- [13] A. Dantan, M. Pinard, *"Quantum-state transfer between fields and atoms in electromagnetically induced transparency"*, Phys. Rev. A **69**, 043810 (2004);
- [14] B. Julsgaard, J. Sherson, J.I Cirac, J. Fiurásek, E.S. Polzik, *"Experimental demonstration of quantum memory for light"*, Nature (London) **432**, 482 (2004)
- [15] A. Dantan, A. Bramati, M. Pinard, *"Atomic quantum memory: Cavity versus single-pass scheme"*, Phys. Rev. A **71**, 043801 (2005).
- [16] J.-Ph. Poizat, J.-F. Roch, and P. Grangier, *"Characterization of Quantum Non-Demolition Measurements in Optics"*, Ann. Phys. (Paris) **19** 265 (1994).
- [17] Arvind, B. Dutta, N. Mukunda and R. Simon, *"The Real Symplectic Groups in Quantum Mechanics and Optics"* quant-ph/9509002 (1995).
- [18] J. Eisert and M. M. Wolf *"Gaussian quantum channels"*, quant-ph/0505151 (2005).
- [19] Lu-Ming Duan, J. I. Cirac, P. Zoller, and E. S. Polzik, *"Quantum Communication between Atomic Ensembles Using Coherent Light"*, Phys. Rev. Lett. **85**, 5643 (2000)

- [20] B. Julsgaard, A. Kozhekin and E. S. Polzik, "Experimental long-lived entanglement of two macroscopic objects" *Nature* **413** 400 (2001).
- [21] S. L. Braunstein and H. J. Kimble, "Teleportation of Continuous Quantum Variables", *Phys. Rev. Lett.* **80**, 869 (1998); S. L. Braunstein, C. A. Fuchs, and H. J. Kimble, "Criteria for continuous-variable quantum teleportation", *J. Mod. Opt.* **47** 267 (2000); T.C. Ralph, P.K. Lam, "Teleportation with bright squeezed light", *Phys. Rev. Lett.* **81**, 5668 (1998); F. Grosshans, Ph. Grangier, "Quantum cloning and teleportation criteria for continuous quantum variables", *Phys. Rev. A (Rapid Comm.)* **64**, 010301(R) (2001)
- [22] I. Devetak and A. Winter, "Relating Quantum Privacy and Quantum Coherence: An Operational Approach" *Phys. Rev. Lett.* **93**, 080501 (2004).
- [23] N. J. Cerf, O. Krüger, P. Navez, R. F. Werner and M. M. Wolf, "Non-Gaussian Cloning of Quantum Coherent States is Optimal", *Phys. Rev. Lett.* **95**, 070501 (2005).
- [24] Wheeler, J. A., "The Past and the Delayed-Choice Double-slit Experiment", in *Mathematical Foundations of Quantum Theory*, ed. Marlow, pp. 9-47, Academic Press, New York, (1978); Miller, W. A. and Wheeler, J. A., "Delayed-Choice Experiments and Bohr's Elementary Quantum Phenomenon", p.140-51. *Proc. Int. Symp. Found. of Quantum Mechs. Tokyo.* (Physical Society of Japan) (1983).
- [25] E. Polzik et al., *Deterministic atom-light quantum interface*, quant-ph/0601186 (2006)
- [26] A.S. Chirkin, A.A. Orlov, D. Yu Parschuk, "Quantum theory of two-mode interactions in optically anisotropic media with cubic nonlinearities: Generation of quadrature- and polarization-squeezed light", *Kvant. Elektron.* **20**, 999 (1993) [*Quantum. Electron.* **23**, 870 (1993)]; N. Korolkova, G. Leuchs, R. Loudon, T.C. Ralph, C. Silberhorn, "Polarization squeezing and continuous-variable polarization entanglement", *Phys. Rev. A* **65**, 052306 (2002); N. Korolkova, R. Loudon, "Nonseparability and squeezing of continuous polarization variables", *Phys. Rev. A* **71**, 032343 (2005)
- [27] Ph. Grangier, J.-M. Courty, S. Reynaud, "Characterization of nonideal quantum non-demolition measurements", *Opt. Comm.*, **89**, 99 (1992); Ph. Grangier, J.-A. Levenson and J.-Ph. Poizat, *Nature* **396**, 537 (1998).
- [28] L. Guidoni, S. Guibal, **T. Coudreau**, B. Dubost, F. Grosshans, *Dynamique d'ions confinés dans un piège de Paul linéaire*, Actes de Coloq9, to be published in *J. Phys. IV*
- [29] P. Rowe, L. Hokenekær, C. Brodersen, M. Drewsen, J. S. Hangst, and J. P. Schiffer "Sympathetic Crystallization of Trapped Ions", *Phys. Rev. Lett.* **82**, 2071 (1999)
- [30] P. R. Fontana, "Spin-Orbit and Spin-Spin Interactions in Diatomic Molecules.. I. Fine Structure of H_2 ", *Pys. Rev.* **125**, 220 (1962).
- [31] J. Ringot, P. Szriftgiser, J. C. Garreau, and D. Delande, "Experimental Evidence of Dynamical Localization and Delocalization in a Quasiperiodic Driven System", *Phys. Rev. Lett.* **85**, 2741 (2000).
- [32] L. Hokenekær and M. Drewsen, "Formation process of large ion Coulomb crystals in linear Paul traps", *Phys. Rev. A* **66**, 013412 (2002).
- [33] B. Roth, A. Ostendorf, H. Wenz, and S Schiller, "Production of large molecular ion crystals via sympathetic cooling by laser-cooled Ba^+ ", *J. Phys. B: At. Mol. Opt. Phys.* **38**, 3673 (2005).
- [34] G. P. Barwood, H. S. Margolis, G. Huang, P. Gill, and H. A. Klein, "Measurement of the Electric Quadrupole Moment of the $4d^2 D_{5/2}$ Level in $^{88}Sr^+$ ", *Phys. Rev. Lett.* **93**, 133001 (2004).
- [35] W. H. Oskay, W. M. Itano, and J. C. Bergquist, "Measurement of the ^{199}Hg $5d^9 6s^2 \ ^2D_{5/2}$ Electric Quadrupole Moment and a Constraint on the Quadrupole Shift", *Phys. Rev. Lett.* **94**, 163001 (2005).
- [36] J.P. Gordon, *Motion in radiation trap*, *Phys. Rev. A* **21**, 1606 (1980)
- [37] A. Lambrecht, T. Coudreau, A.M. Steinberg, E. Giacobino, *Europhys. Lett.* **36**, 93 (1996)
- [38] W. Paul, *Electromagnetic traps for charged and neutral particles*, *Rev. Mod. Phys.* **62**, 3 (1990)
- [39] M.G. Raizen, J.M. Killigan, J.C. Bergquist, W. M. Itano, D.J. Wineland, *Phys. Rev. A* **45**, 6493 (1992)